DEPARTMENT OF DEFENCE

DEFENCE SCIENCE AND TECHNOLOGY ORGANISATION

AERONAUTICAL RESEARCH LABORATORIES

MELBOURNE, VICTORIA

STRUCTURES REPORT 400

AD-A145 991

STRAINS IN AN ELASTIC PLATE CONTAINING AN INTERFERENCE-FIT BOLT NEAR A FREE EDGE

by

G. S. JOST and R. P. CAREY

DTIC

APPROVED FOR PUBLIC RELEASE

SEP 2 7 1984

E

DTIC FILE COPY

COPY No

AR-003-012

DEPARTMENT OF DEFENCE
DEFENCE SCIENCE AND TECHNOLOGY ORGANISATION
AERONAUTICAL RESEARCH LABORATORIES

STRUCTURES REPORT 400

STRAINS IN AN ELASTIC PLATE CONTAINING AN INTERFERENCE-FIT BOLT NEAR A FREE EDGE

by

G. S. JOST and R. P. CAREY

SUMMARY

An approximation has been developed to permit the use of elastic theory for a pressurized hole near the edge of a semi-infinite plate to predict strains in one containing an interference-fit fastener. A comparison of measured plate strains with those predicted for such a situation shows good agreement.

CONTENTS

1. INTRODUCTION

Various techniques, including the use of interference-fit fasteners, have been developed in recent years for improving the fatigue performance of bolted joints, Although such fasteners are now used extensively in modern civil and military aircraft, the basis for their adoption rests almost wholly upon experimentally observed improvements in fatigue behaviour. Theoretical support or understanding for this demonstrated improvement remains largely qualitative.

Uncertainties in the stress/strain fields around the Taper-Lok interference-fit fasteners used in the F-111C aircraft led to the experimental work reported here and elsewhere.[1] Whereas solutions for elastic stress and strain fields around a hole containing an interference fastener in a large plate are readily available, the presence of nearby boundaries causes considerable theoretical difficulty.

For the present case of a hole near the edge of a semi-infinite plate containing an interference-fit fastener, an approximation has been developed from the exact, related elastic theory for a pressurized hole in a geometrically similar plate. Strains predicted from this theory have been compared with measured experimental strains.

2. ELASTIC ANALYSIS

2.1 Pressurized Hole in a Semi-Infinite Plate

The elastic stresses in a semi-infinite plate containing a pressurized hole were derived by Jeffery[2] in his general study of problems in which the use of bipolar coordinates was particularly effective. They are as follows:

$$\sigma_\alpha/p = -M\{(\cosh \alpha - \cos \beta)2 \cosh \alpha_1 \sinh \alpha + 2 \sinh \alpha \cos \beta \cosh(2\alpha - \alpha_1) \\ -\sinh \alpha_1 - \sinh(2\alpha - \alpha_1)\} \tag{1}$$

$$\sigma_\beta/p = M\{(\cosh \alpha - \cos \beta)[2 \cosh \alpha_1 \sinh \alpha + 4 \sinh(2\alpha - \alpha_1)\cos \beta] \\ -2 \sinh \alpha \cos \beta \cosh(2\alpha - \alpha_1) + \sinh \alpha_1 + \sinh(2\alpha - \alpha_1)\} \tag{2}$$

$$\tau_{\alpha\beta}/p = -2M(\cosh \alpha - \cos \beta)[\cosh \alpha_1 - \cosh(2\alpha - \alpha_1)]\sin \beta \tag{3}$$

where

$$M = \tfrac{1}{2} \operatorname{cosech}^3 \alpha_1$$

and

$$\alpha_1 = \operatorname{arcosh} d/r. \tag{4}$$

The nomenclature of the bipolar coordinate system is illustrated in Fig. 1. Near the hole, σ_α corresponds to the 'radial' stress, and σ_β to the 'hoop' stress. Cartesian coordinates x, y shown in Fig. 1 are related to bipolar coordinates thus:

$$x = a \sin \beta/(\cosh \alpha - \cos \beta)$$

$$y = a \sinh \alpha/(\cosh \alpha - \cos \beta)$$

$$a^2 = d^2 - r^2$$

1

Stresses in the x, y directions are found from:

$$\sigma_x = \tfrac{1}{2}(\sigma_\beta + \sigma_\alpha) + \tfrac{1}{2}(\sigma_\beta - \sigma_\alpha)\cos 2\theta + \tau_{\alpha\beta}\sin 2\theta \tag{5}$$

$$\sigma_y = \tfrac{1}{2}(\sigma_\beta + \sigma_\alpha) - \tfrac{1}{2}(\sigma_\beta - \sigma_\alpha)\cos 2\theta - \tau_{\alpha\beta}\sin 2\theta \tag{6}$$

where

$$\theta = \pm \arcsin\left\{\frac{\sinh\alpha\,\sin\beta}{\cosh\alpha - \cos\beta}\right\}$$

unless

$$(y^2 - a^2 - x^2)/y > 0$$

when

$$\theta = \pi \mp \arcsin\left\{\frac{\sinh\alpha\,\sin\beta}{\cosh\alpha - \cos\beta}\right\}.$$

The upper signs of these equations apply when x is positive, the lower signs when x is negative.

For predicting strains in the plate, plane stress conditions have been adopted. The strains are therefore found from:

$$\epsilon_x = \frac{1}{E_p}\left\{\sigma_x - \nu_p\,\sigma_y\right\} \tag{7}$$

and

$$\epsilon_y = \frac{1}{E_p}\left\{\sigma_y - \nu_p\,\sigma_x\right\} \tag{8}$$

where ν_p is Poisson's ratio for the plate material and E_p is Young's modulus.

2.2 Relation Between Interface Pressure and Interference

Interference-fit bolts give rise to interface pressure between the bolt surface and the hole and hence to stresses and strains in both the plate and bolt. In axisymmetric situations, such as that of a hole in an infinite plate or a thick-walled cylinder, exact relations between the *uniform* pressure generated and the interference may be readily found. In the present case, however, interference fits do not result in a uniform interface pressure and so theory based upon the application of a uniform pressure in the hole cannot be directly applicable. The theory can, however, be used to effect in an approximate way to calculate the *average* radial expansion of the hole (together with the corresponding radial contraction of the bolt) and so relate interference with average interface pressure. The latter can then be used as required in the preceding formulae.

In deriving the required relationship between interface pressure and interference, plane stress conditions are assumed for the plate, and plane strain for the bolt. The average radial expansion of the hole, u_p, is found by evaluating the total increase in the circumference of the hole under the action of the pressure p and dividing this by 2π. Thus, u_p is found from

$$u_p = \frac{1}{2\pi}\int_0^{2\pi} r\,\epsilon_\beta\,d\psi \tag{9}$$

where $d\psi$ is an elemental angle from the hole centre.

For plane stress conditions in the plate

$$E_p\,\epsilon_\beta = \sigma_\beta - \nu_p\,\sigma_\alpha \tag{10}$$

2

where subscript p refers to the plate and σ_α and σ_β on the bore of the hole are found from (1) and (2) as

$$\sigma_\alpha = -p \tag{11}$$

and

$$\sigma_\beta = p[2(\cosh^2 \alpha_1 - \cos^2 \beta)\operatorname{cosech}^2 \alpha_1 - 1] \tag{12}$$

To permit integration of (12), $\cos^2 \beta$ must be expressed in terms of θ. Referring to Fig. 1, application of the sine rule to ABC results in

$$\tan \phi = \frac{\sin \psi}{(d/r) - \cos \psi}.$$

In addition, in Ref. 2 it is shown that

$$\tan \phi = (r/a)\sin \beta$$

Equating these expressions and rearranging gives

$$\cos^2 \beta = 1 - \left\{\left(\frac{a}{r}\right)^2 \sin^2 \psi\right\} \bigg/ \left(\frac{d}{r} - \cos \psi\right)^2$$

Substituting (11) and (12) into (10) and performing the integration in (9) yields*

$$u_p = \frac{pr}{E_p}\left(1 + \nu_p\right)\left[1 + \frac{2(\coth \alpha_1 - 1)}{1 + \nu_p}\right] \tag{13}$$

where the term in square brackets represents the semi-infinite plate correction to the infinite plate solution.

For the bolt under the same pressure p, the (uniform) change in radius is readily found from

$$u_b = r\epsilon_\beta \tag{14}$$

and the plane strain condition from

$$E_b\epsilon_\beta = (1 + \nu_b)[(1 - \nu_b)\sigma_\beta - \nu_b\sigma_\alpha]. \tag{15}$$

On the surface of the bolt

$$\sigma_\alpha = \sigma_\beta = -p \tag{16}$$

and hence the displacement is given by†

$$u_b = -\frac{pr}{E_b}\left(1 + \nu_b\right)\left(1 - 2\nu_b\right). \tag{17}$$

The sum of the moduli of the displacements u_p and u_b must equal the interference between bolt and plate, so that in terms of a dimensionless interference λ defined by

$$\lambda = \frac{|u_p| + |u_b|}{r},$$

$$\lambda = \frac{p}{E_p}\left(2 \coth \alpha_1 + \nu_p - 1\right) + \frac{p}{E_b}\left(1 + \nu_b\right)\left(1 - 2\nu_b\right). \tag{18}$$

---

* The corresponding formulation for plane strain conditions in the plate is

$$u_p = \frac{pr}{E_p}\left(1 + \nu_p\right)\left[1 + 2\left(1 - \nu_p\right)\left(\coth \alpha_1 - 1\right)\right].$$

† For a bolt in plane stress, (17) becomes

$$u_b = -\frac{pr}{E_b}\left(1 - \nu_b\right).$$

Thus, for given λ and knowing the elastic parameters of plate and bolt, the average interface pressure p may be determined from (18) and used as required in eqns (1) to (8).

2.3 Onset of Yielding

In the experimental program to be described, the Taper-Lok interference-fit fasteners eventually caused yielding of the plate material. It is necessary, therefore, in this elastic analysis to ascertain the location of the onset of yielding and the stage at which it occurs, so that post-yield experimental data should be excluded from this analysis.

With increasing interference yielding will occur at the hole boundary where the elastic principal stresses are given by (11) and (12). For plane stress, the von Mises yield criterion becomes

$$\sigma_\alpha{}^2 + \sigma_\beta{}^2 - \sigma_\alpha\sigma_\beta = \sigma_y{}^2 \tag{19}$$

where σ_y is the uniaxial yield stress of the plate material. Substitution of (11) into (19) yields

$$\left(\frac{\sigma_\beta}{p}\right)^2 + \frac{\sigma_\beta}{p} + 1 = \left(\frac{\sigma_y}{p}\right)^2 \tag{20}$$

from which the value of β which maximises σ_β provides the required solution. It is, from (12),

$$\beta = \pm\frac{\pi}{2} \tag{21}$$

when the limiting (elastic) tangential stress becomes, from (12)

$$\sigma_\beta/p = 2\coth^2\alpha_1 - 1. \tag{22}$$

3. EXPERIMENTAL PROGRAM

3.1 Test Specimens

Two specimen configurations were used. Specimen C, illustrated in Fig. 2(a), was a simple square plate with a single tapered hole approximately $1\cdot5$ diameters from an edge. The specimens identified as 4/5 and 6/7 and shown in Fig. 2(b) were rectangular with thickened lug ends and each contained two tapered holes, similarly approximately $1\cdot5$ diameters one from each edge. All holes were finished with an 18 flute tungsten carbide reamer.

The specimen material was D6ac steel heat treated to achieve an ultimate tensile stress in the range 1510 to 1650 MPa. The stress–strain characteristics of the material of specimen C are shown in Fig. 5.

The tapered bolts fitted into the reamed holes were of the Taper-Lok type, Code 2TLHC2-6, and of nominal diameter 3/8 inch ($9\cdot525$ mm). They were manufactured from H11 steel and had a nickel–cadmium plating with a wax-like coating of cetyl alcohol. The taper of one in 48 allowed accurate increments in interference to be calculated from measured increments in insertion distance.

Numerous short gauge length electric resistance strain gauges were bonded to the specimens near the holes on both the faces and edges of the specimens. The gauge types are given in Table 1. Their locations are shown in Fig. 2(a) (specimen C), Fig. 3 (specimen 4/5) and Fig. 4 (specimen 6/7). With the exception of those gauges located on the specimen edges, the gauges were bonded on the faces from which the bolts were inserted in the holes.

3.2 Test Procedure

Each tapered bolt was inserted with firm thumb pressure while the specimen was clamped along one side in a vice. Interference was increased in steps of approximately $0\cdot01$ mm on diameter by tightening the nuts. Strains and insertion distances were measured—the latter by a depth micrometer from displacements of the bolt head. Tables 2, 3 and 4 give the values recorded for each specimen.

4

The process was continued to 0·064 mm interference on diameter in the case of specimen 4/5 and considerably higher in specimens C and 6/7. Only data collected within the elastic regime are presented here.

3.3 Errors in Strain

Some of the gauges used had a relatively large grid dimension in one direction. Because of the strain gradients around the holes introduced by the interference-fit fasteners errors in strain arise as follows:

(a) For gauges that are long in the radial direction, the average strain over the radial dimension differs from the strain at the centre of the gauge.

(b) For gauges long in the circumferential direction, the grid near the ends is not truly aligned in the circumferential direction.

(c) For the same type of gauge, edge distance is increasingly in error near the ends.

For type (a) errors it can be shown by integration over the gauge length that, for strains distributed as $1/r^2$, the fractional error in strain at the gauge centre is given by

$$g^2/(c^2 - g^2)$$

where g is the half gauge dimension in the radial direction and c is the distance from hole centre to the gauge centre. The error for a 1·8 mm long gauge, 1·21 mm from the hole, was found to be $+2·2\%$, the maximum for errors of type (a).

Misalignment errors (type (b)) were averaged for 5 positions across one side of a gauge, using Mohr's circle to estimate the individual deviations. The largest error from this cause was $-1·9\%$ for the case of a 1·8 mm long gauge located 0·51 mm from the hole. Edge distance errors (type (c)) were also averaged on a point to point basis along the gauge. For the example just given the error from this cause was found to be $-1·0\%$.

In summary, the total error from the three causes for the 1·8 mm gauge length circumferentially aligned 0·51 mm from the hole was $-2·8\%$; total error for 1·8 mm gauge radially aligned was estimated to be $+2·2\%$; and for gauges of dimension $0·38 \times 0·51$ mm the error from these causes was less than 1%.

4. COMPARISON OF MEASURED AND PREDICTED STRAINS

Because the experimental strain data covered both the elastic and plastic regimes, it was necessary, for the present elastic analysis, to ascertain the interference beyond which plastic flow at the hole begins. Experimental data in the plastic region were then excluded from subsequent consideration. The upper limit of the elastic regime was established as follows:

4.1 Estimation of Yield Incipience

As the initial stage of pin insertion often induces a non-linear response in the specimen, strain level rather than insertion distance was used to determine yield incipience. For this purpose the strain gauge nearest to each hole was adopted as control gauge. The strain corresponding to this condition was computed theoretically for the relevant gauges and used to define the upper limits of insertion for which valid estimates of elastic strains could be derived.

In more detail, σ_y/p at incipience was evaluated using equations (4), (20) and (22). With σ_y estimated from Fig. 5 as 1150 MPa, the interface pressures p were calculated to be 588 MPa (for specimen C) and 585 MPa (specimens 4/5 and 6/7). (The corresponding limiting values of

non-dimensional interference were 0·00552 and 0·00551). The critical strain level at the control gauges was then found from equations (1) to (8) using common values of elastic parameters for both bolt and plate of $E = 207 \times 10^3$ MPa and $\nu = 0 \cdot 3$.

4.2 Comparison of Theory and Experiment

The measured (elastic) strains listed in Tables 2, 3 and 4 for the three specimens are shown plotted in Figs 6 to 11 against bolt insertion distance. Best fit straight lines are also shown. In some cases the lowest strain readings have not been included in the analysis because of evident inconsistency with remaining data arising, possibly, from bolt/hole imperfections.

The slopes of the fitted lines represent strain per unit bolt insertion distance. These are readily converted to strain per unit (dimensionless) interference, and in this form are listed in Table 5. They have also been plotted against non-dimensional edge distance for two radial traverses— perpendicular to and parallel with the nearest specimen edge—in Figs 12 and 13 for the single hole specimen and in Figs 14 and 15 for the double hole specimens.

The theoretical curves shown in Figs 12 to 15 have been calculated using equations (1) to (8) together with equation (18), selected values being given in Table 6.

5. DISCUSSION

Figures 12 to 15 inclusive show the agreement between predicted and measured strains to be good. Some differences are apparent for radial strains in the high strain gradient region close to the hole, but the reasons for this cannot be identified.

The overall substantial agreement noted above indicates that the approximation developed to relate average bolt/hole interface pressure to interference for the present non-axisymmetric case is quite successful*. The approximation must improve as the hole becomes more remote from the plate edge, but it must also be expected to begin to break down as the hole becomes closer to the edge. The present study provides no indication as to when this might be expected to occur.

CONCLUSIONS

An approximation has been developed to permit the use of elastic theory for a pressurized hole near the edge of a semi-infinite plate to predict strains in one containing an interference-fit fastener. A comparison of measured plate strains and those predicted for a Taper-Lok inter-ference-fit installation shows good agreement.

---

* Another successful application of the approximation to a plane strain situation is reported in Appendix 5 of Ref. 3.

REFERENCES

1. Carey, R. P.   Experimental determinations of strain fields resulting from inter- ference-fit tapered pins. *Dept. Supply, Aeronautical Res. Labs.* Structures and Materials Note 377, June 1972.

2. Jeffery, G. B.   Plane stress and plane strain in bipolar coordinates. Phil. Trans. Roy. Soc. Series A, v. 221, 1921, pp. 265–293.

3. Mann, J. Y., Revill, G. W., and Lupson, W. F.   Improving the fatigue performance of thick aluminium alloy bolted joints by hole cold-expansion and the use of interference-fit steel bushes. *Dept. Defence, Aeronautical Res. Labs.* Structures Note 486, April 1983.

TABLE 1

Electric Resistance Strain Gauges

Gauge Type	Specimen	Orientation Relative to Hole	Position	Gauge Length mm	Width mm
'Micromeasurements' EA–06–015–DJ–120	6/7	Circumferential	Near tapered hole 7	0·38	0·51
	4/5	Circumferential	Near hole 5 on traverse perpendicular to longitudinal axis	0·38	0·51
'Micromeasurements' WA-06-125-BT-120	6/7 and 4/5	Longitudinal	Specimen edge		
'Kyowa' KFC-03-C1-11	6/7	Radial	Near holes 6 and 7	0·3	1·
	4/5	Radial	Near holes 4 and 5 on longitudinal direction traverses	0·3	1·ᴜ
		Circumferential	As above	0·3	1·8
'Kyowa' KF-03-C1-11	C	Longitudinal	Specimen edge		
'Shinkoh' FIP 55-30	4/5	Radial	Near hole 4 on traverse perpendicular to longitudinal axis	0·5	1·5
'Metal film' C6-1 × 1-MI5E	C	Circumferential	Near hole	0·38	0·51

Bonding used: M Bond 200 with catalyst.

TABLE 2

Strains* Resulting from Insertion of Tapered Bolts—Single Hole Specimen C

Gauge	Bolt Insertion Distance (mm)				
	0·90	1·27	1·70	1·96	2·58
1	0·506	0·762	0·960	1·162	1·482
2	1·025	1·580	2·019	2·330	3·043
3	0·922	1·498	1·829	2·230	2·801
4	0·814	1·339	1·546	1·999	2·788

* $\times 10^{-3}$

TABLE 3

Strains* Resulting from Insertion of Tapered Bolts—Specimen 4/5

Gauge	Bolt Insertion Distance (mm)						
	Thumb Tight	0·48	0·99	1·60	2·03	2·57	3·05
1	0·022	0·229	0·450	0·765	1·039	1·304	1·545
2	0·002	0·122	0·347	0·693	1·009	1·311	1·578
3	−0·055	0·226	0·654	1·269	1·839	2·389	2·816
4	−0·006	0·223	−0·444	−1·163	−1·719	−2·342	−2·947
5	−0·016	0·169	0·604	1·072	1·538	1·994	2·410
6	−0·004	0·157	0·617	1·277	1·816	2·359	2·909
7	0·004	0·136	0·450	0·851	1·206	1·579	1·940
8	0·000	0·094	0·299	0·568	0·808	1·056	1·294
	Thumb Tight	0·51	1·02	1·47	1·96	2·44	
9	−0·002	−0·130	−0·285	−0·454	−0·623	−0·831	
10	−0·002	−0·182	−0·416	−0·681	−0·959	−1·275	
11	0·002	−0·314	−0·834	−1·440	−2·083	−2·714	
12	0·000	−0·076	−0·645	−1·135	−2·004	−2·615	
13	0·008	0·238	0·536	0·964	1·239	1·761	
14	−0·093	−0·373	−0·951	−1·450	−1·878	−2·325	
15	0·012	0·209	0·463	0·698	0·947	1·214	

* × 10⁻³.

TABLE 4

Strains* Resulting from Insertion of Tapered Bolts—Specimen 6/7

Gauge	Bolt Insertion Distance (mm)					
	Thumb Tight	0·66	1·19	1·85	2·24	2·79
1	0·002	0·281	0·521	0·893	1·125	1·412
2	−0·004	0·190	0·414	0·797	1·022	1·265
3	−0·006	0·265	0·590	1·110	1·440	1·765
4	0·000	0·290	0·721	1·553	2·021	2·475
5	0·002	0·543	1·066	1·544	2·216	2·809
6	0·002	0·304	0·660	0·988	1·400	1·758
7	0·000	−0·314	−0·607	−1·674	−2·016	−2·883
8	0·000	0·500	0·896	1·658	2·099	2·760
9	0·000	0·357	0·616	1·088	1·353	1·750
	Thumb Tight	0·97	1·32	1·83	2·29	2·92
10	−0·002	−0·223	−0·381	−0·544	−0·712	−0·858
11	−0·002	−0·194	−0·727	−1·207	−1·898	−2·449

* $\times 10^{-3}$.

TABLE 5

Measured Strain per Unit Interference Ratio

Specimen	Gauge Number	Non-dimensional position[1]	Strain/ Unit interference ratio[2]
C	1	2·99	0·269
	2	1·11	0·549
	3	1·16	0·512
	4	1·10	0·531
4/5	1	2·93	0·251
	2	1·66	0·283
	3	1·16	0·501
	4	1·10	−0·566
	5	1·29	0·411
	6	1·14	0·520
	7	1·42	0·340
	8	1·72	0·228
	9	1·81	−0·178
	10	1·51	−0·281
	11	1·18	−0·618
	12	1·14	−0·669
	13	1·25	0·389
	14	1·18	−0·448
	15	2·93	0·247
6/7	1	2·93	0·262
	2	1·82	0·251
	3	1·49	0·348
	4	1·16	0·520
	5	1·16	0·524
	6	1·46	0·330
	7	1·13	−0·651
	8	1·15	0·543
	9	1·46	0·331
	10	1·77	−0·152
	11	1·14	−0·543

[1] Ratio of distance from hole centre/hole radius.

[2] Positive readings are from circumferential gauges. Negative readings are from radial gauges.

TABLE 6

Theoretical Strain per Unit Interference Ratio

Edge distance ratio[1]	Non-dimensional position[2]	Strain/Unit interference ratio	
		Circumferential	Radial
Traverse Perpendicular to Plate Edge (refer Fig. 12)			
2·99	2·99 (Plate edge)	0·259	
	2·5	0·208	
	2·0	0·228	
	1·5	0·340	
	1·0 (Hole)	0·669	
	−1·0 (Hole)	0·669	
	−1·5	0·305	
	−2·0	0·171	
Traverse Parallel to Plate Edge (refer Fig. 13)			
2·99	1·0 (Hole)	0·784	
	1·25	0·483	
	1·5	0·310	
	2·0	0·135	
Traverse Perpendicular to Plate Edge (refer Fig. 14)			
2·93	2·93 (Plate edge)	0·271	−0·081
	2·5	0·219	−0·081
	2·0	0·233	−0·138
	1·4	0·382	−0·332
	1·0 (Hole)	0·667	−0·667
	−1·0 (Hole)	0·667	−0·667
	−1·5	0·304	−0·292
	−2·0	0·171	−0·155
Traverse Parallel to Plate Edge (refer Fig. 15)			
2·93	1·0 (Hole)	0·787	−0·703
	1·2	0·532	−0·461
	1·4	0·369	−0·308
	2·0	0·134	−0·091
	3·0	0·020	−0·005

[1] Ratio of hole centre to edge distance/hole radius (2·99 for specimen C, 2·93 for specimens 4/5 and 6/7).

[2] Ratio of distance from hole centre/hole radius.
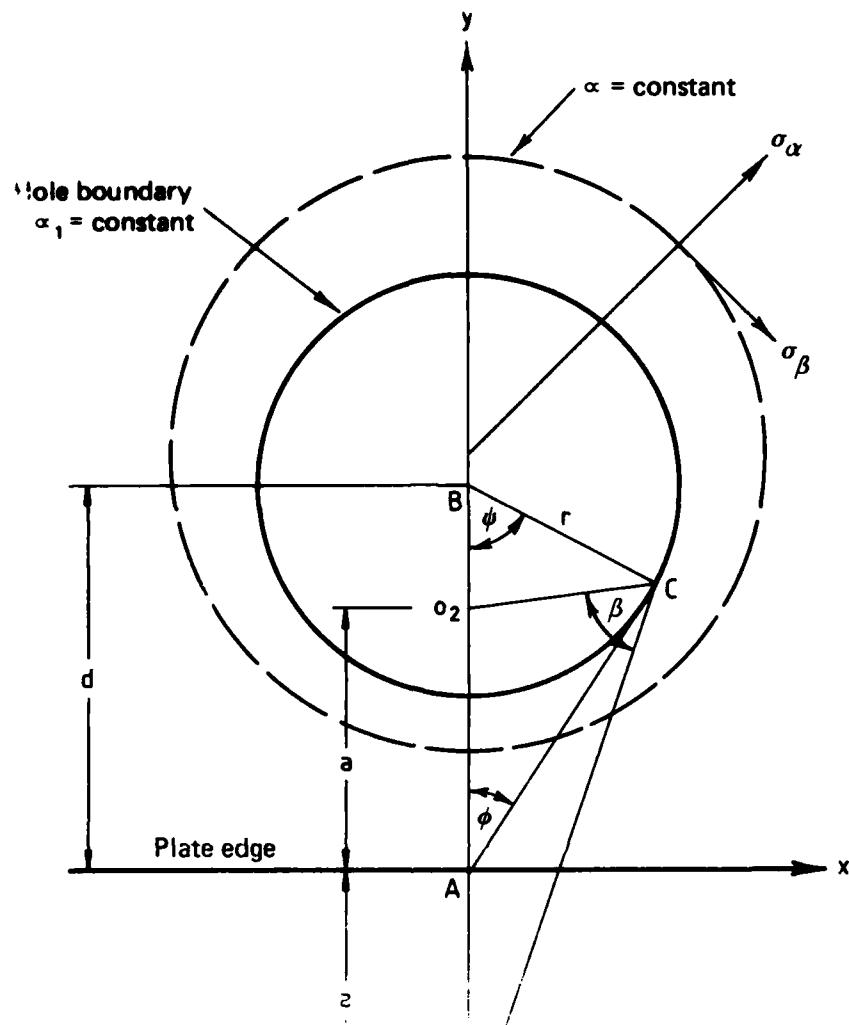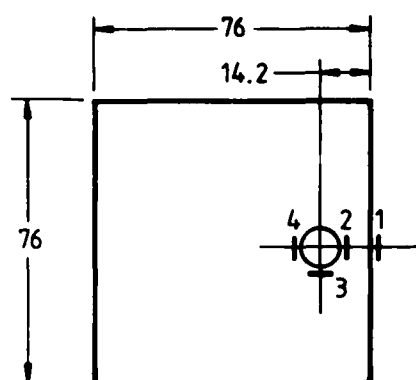
Gauge No.	Centreline Distance from hole edge (mm)
1	0.64
2	0.51
3	0.79
4	0.48

Hole taper-reamed to suit
9.525mm nominal diameter
taper-lok bolt

Plate thickness = 4.72mm

FIG. 2 (a)   CONFIGURATION AND GAUGE LOCATIONS –
             SPECIMEN C

Holes taper-reamed to suit
9.525mm nominal diameter
taper-lok bolt
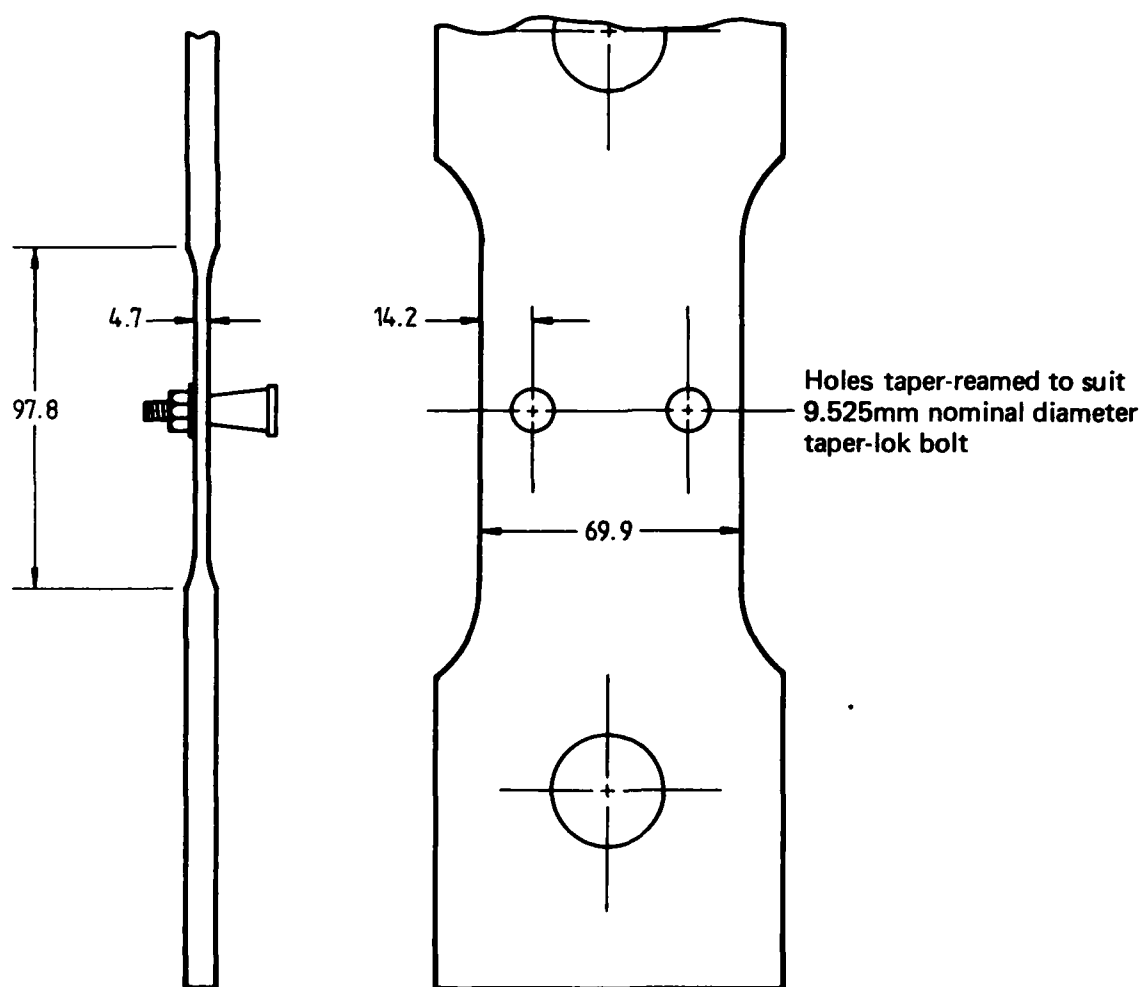
All dimensions in mm

FIG. 2 (b)   CONFIGURATION OF SPECIMENS 4/5 AND 6/7
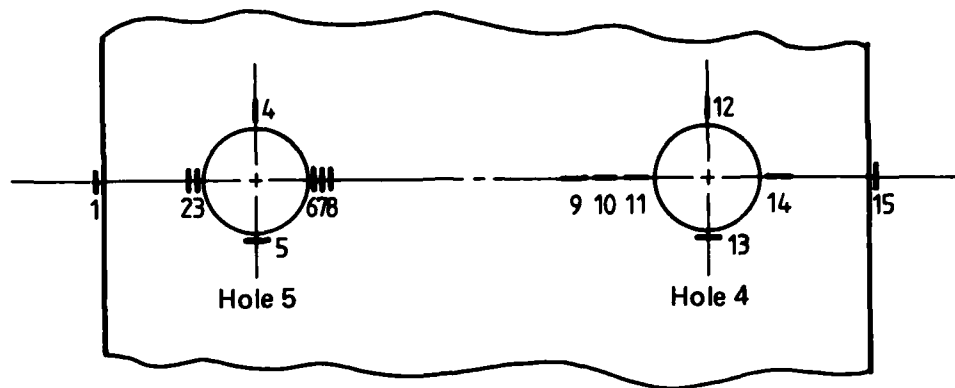
Centreline distance from hole edge (mm)

Gauge No. 1	—	9.40		Gauge No. 9	—	3.94
2	—	3.20		10	—	2.51
3	—	0.79		11	—	0.89
4	—	0.51		12	—	0.69
5	—	1.42		13	—	1.206
6	—	0.66		14	—	0.89
7	—	2.03		15	—	9.40
8	—	3.53				

FIG. 3   GAUGE LOCATIONS ON SPECIMEN 4/5 —
REFER FIG. 2 (b)
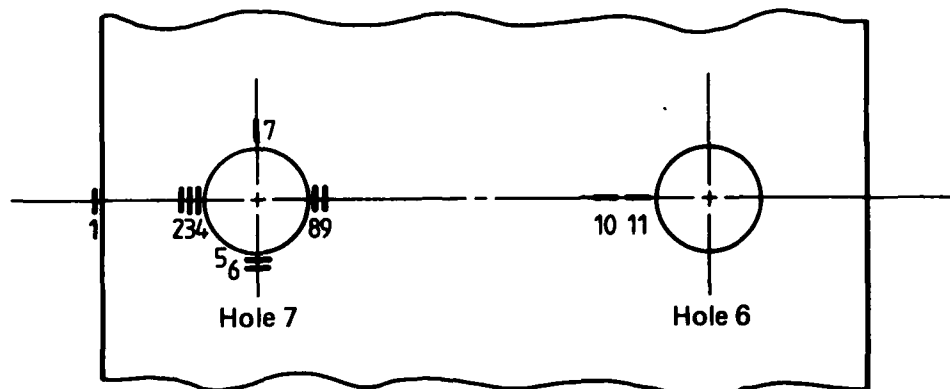
Centreline distance from hole edge (mm)

Gauge No. 1	—	9.40		Gauge No. 6	—	2.23
2	—	4.00		7	—	0.62
3	—	2.37		8	—	0.72
4	—	0.77		9	—	2.25
5	—	0.77		10	—	3.76
				11	—	0.66

FIG. 4   GAUGE LOCATIONS ON SPECIMEN 6/7 —
REFER FIG. 2 (b)
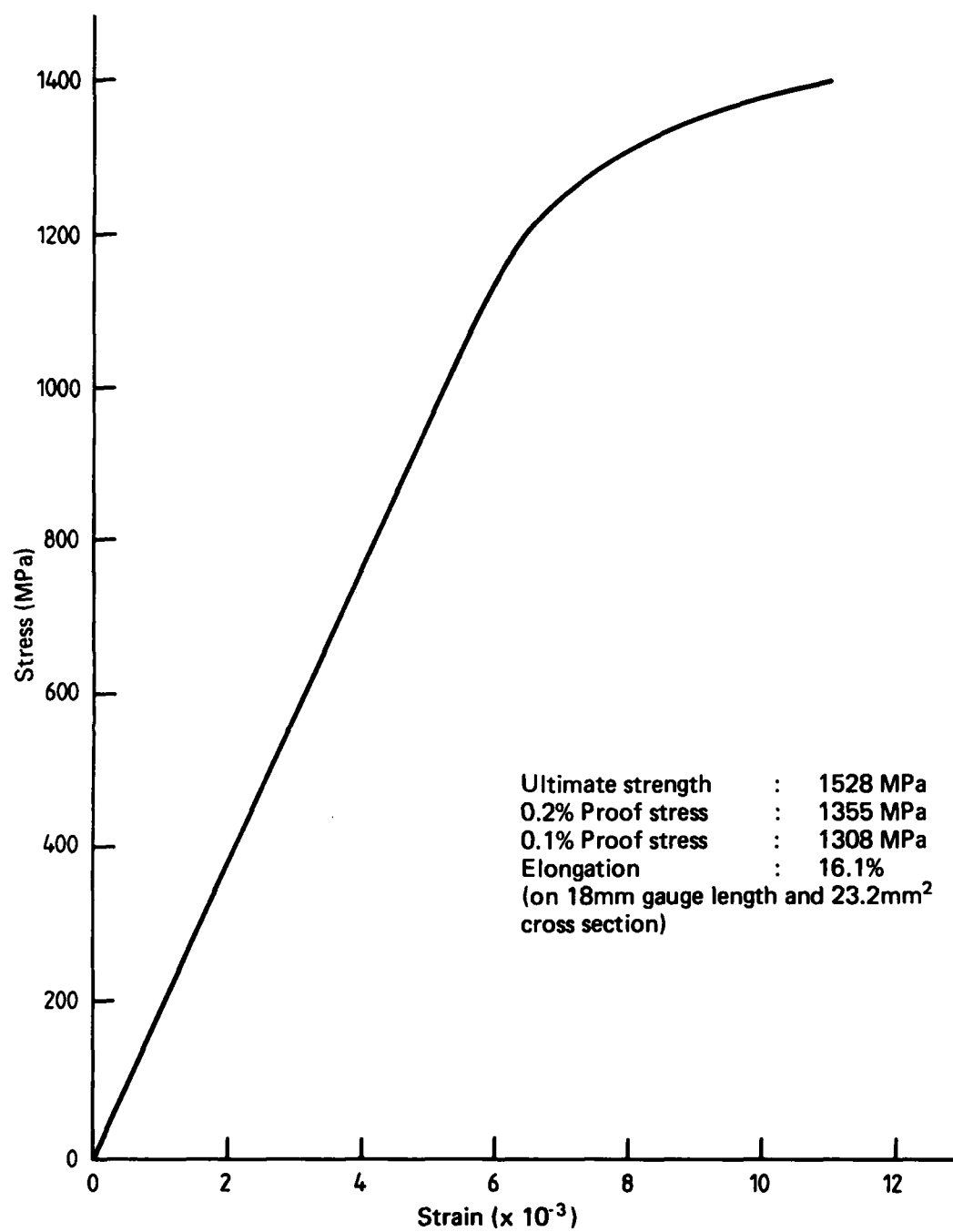
FIG. 5   STRESS – STRAIN CHARACTERISTICS FOR
D6 ac MATERIAL
Material of specimen C
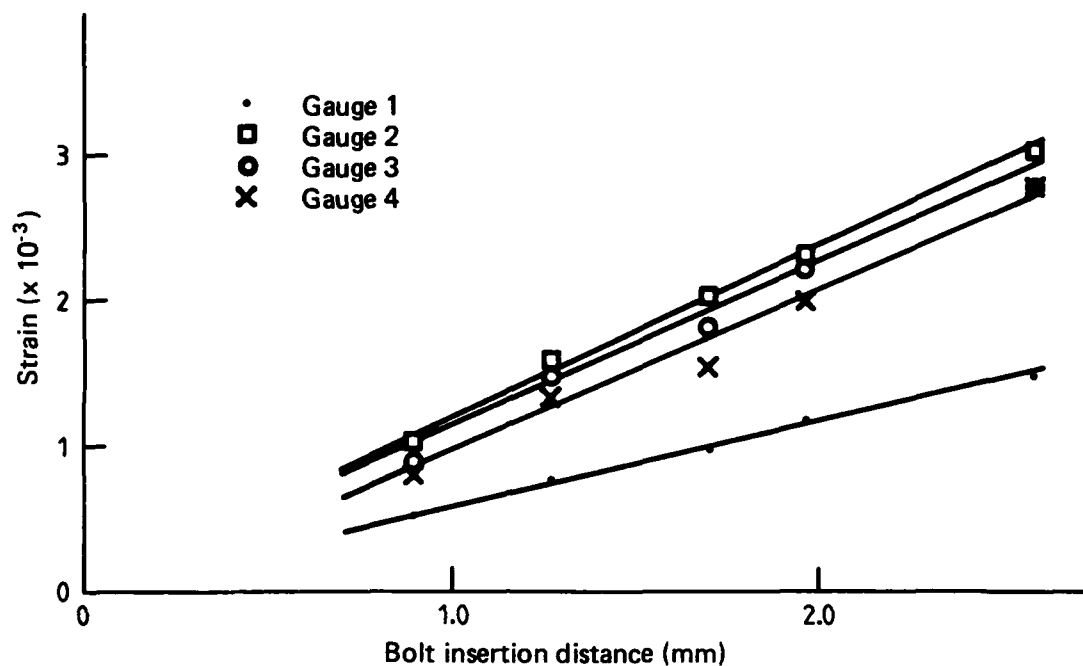
FIG. 6   STRAIN VERSUS INSERTION DISTANCE —
SPECIMEN C
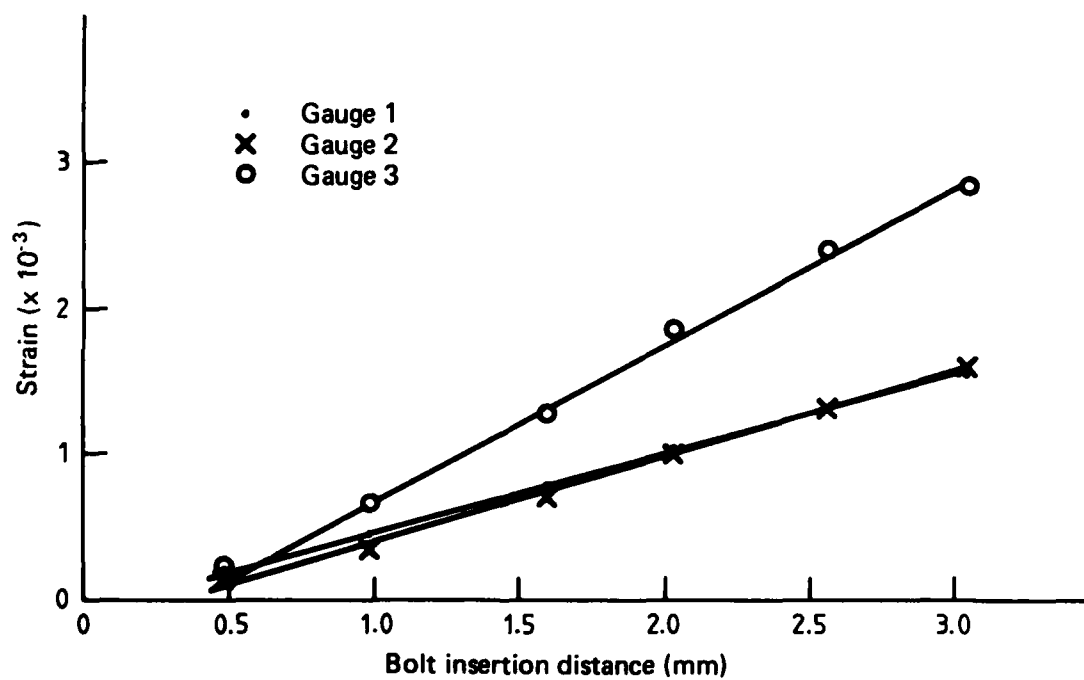
FIG. 7   STRAIN VERSUS INSERTION DISTANCE —
SPECIMEN 4/5
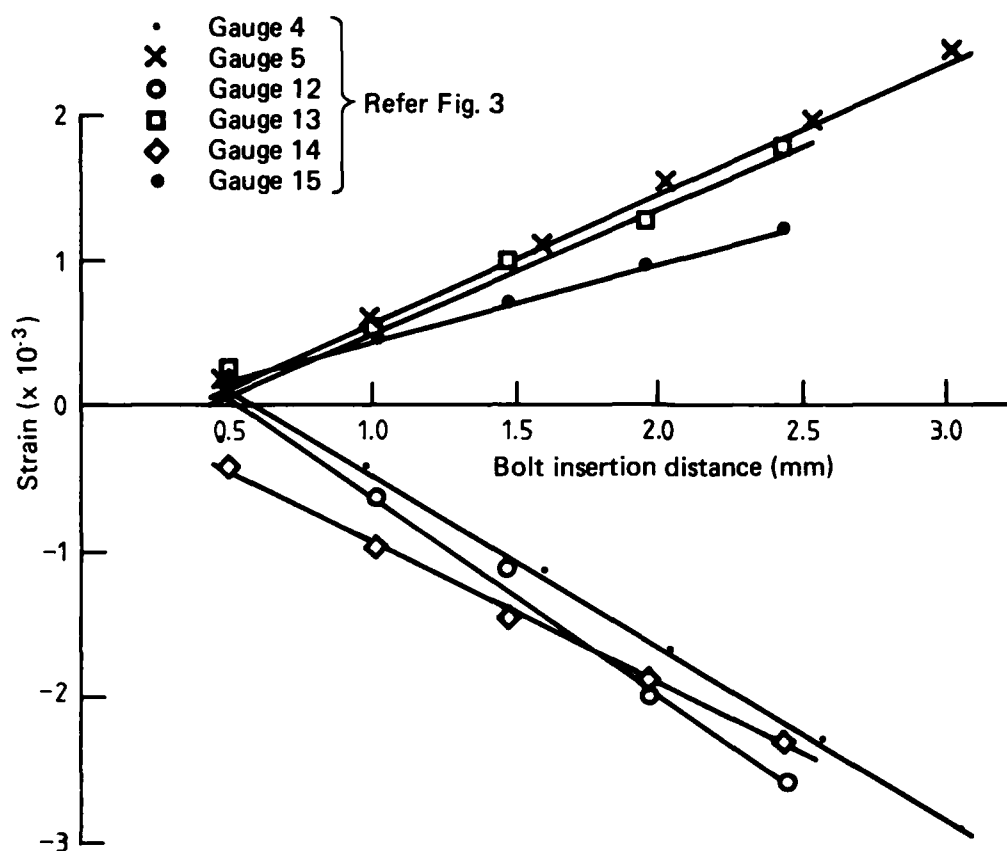
FIG. 8 STRAIN VERSUS INSERTION DISTANCE —
SPECIMEN 4/5
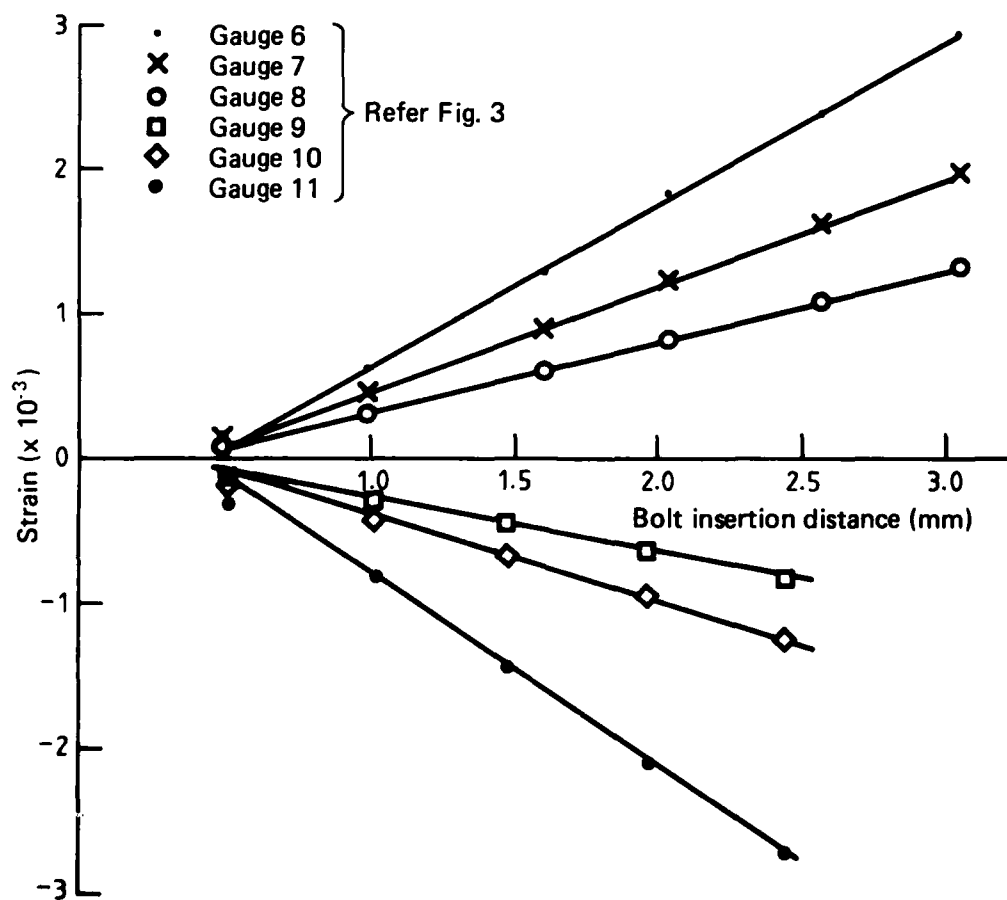
FIG. 9 STRAIN VERSUS INSERTION DISTANCE —
SPECIMEN 4/5
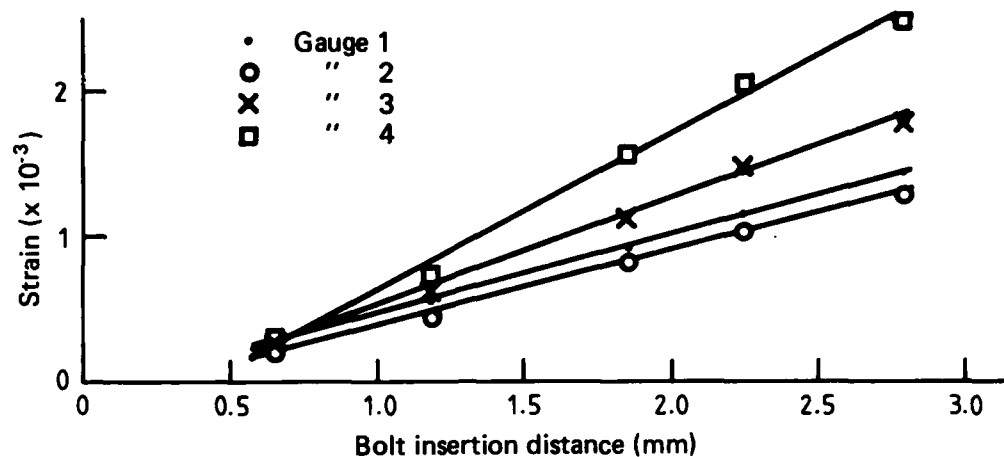
FIG. 10   STRAIN VERSUS INSERTION DISTANCE —
SPECIMEN 6/7
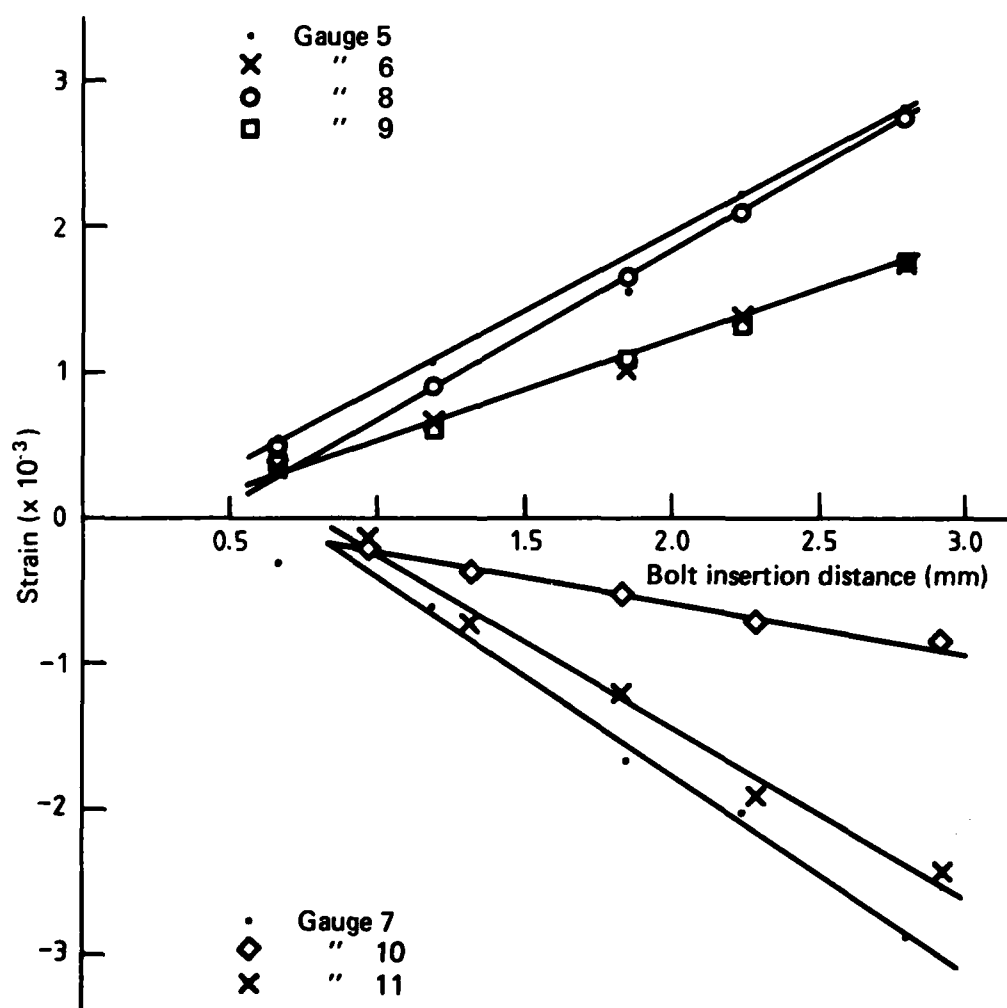
FIG. 11   STRAIN VERSUS INSERTION DISTANCE —
SPECIMEN 6/7
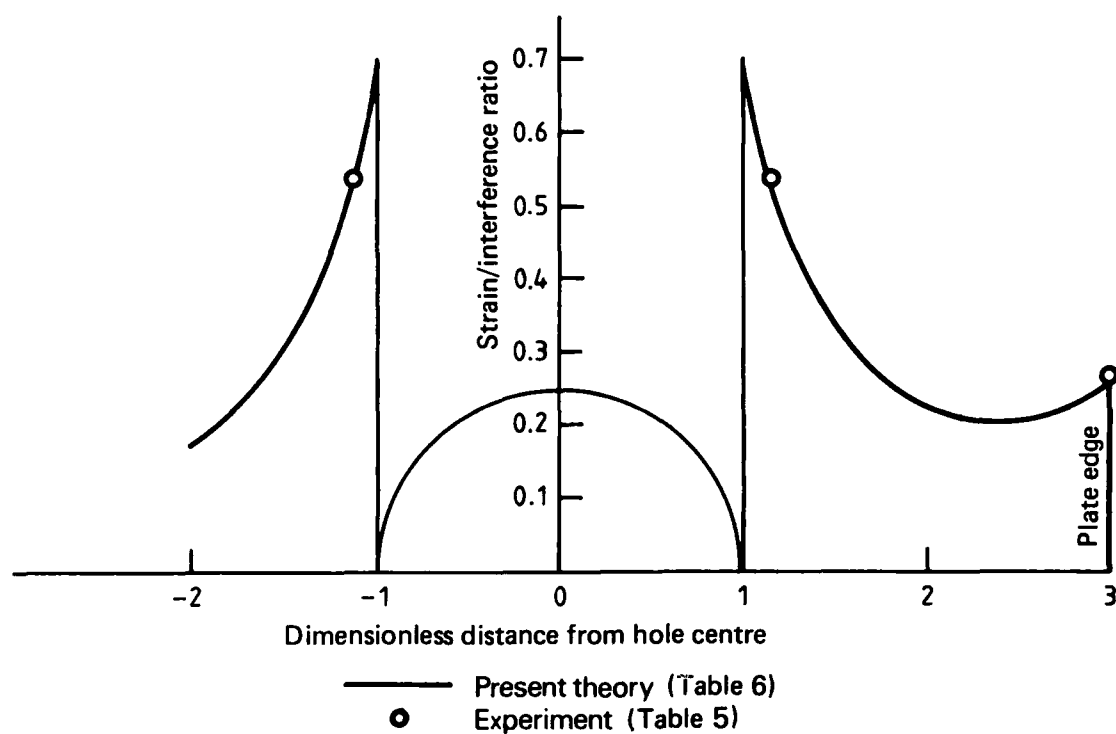
FIG. 12   STRAIN TRAVERSE PERPENDICULAR TO SPECIMEN EDGE --
CIRCUMFERENTIAL STRAINS IN SINGLE-HOLE SPECIMEN C

FIG. 13   STRAIN TRAVERSE PARALLEL TO SPECIMEN EDGE --
CIRCUMFERENTIAL STRAINS IN SINGLE-HOLE SPECIMEN C

Strain/interference ratio

Circumferential strain

Plate edge

Dimensionless distance from hole centre
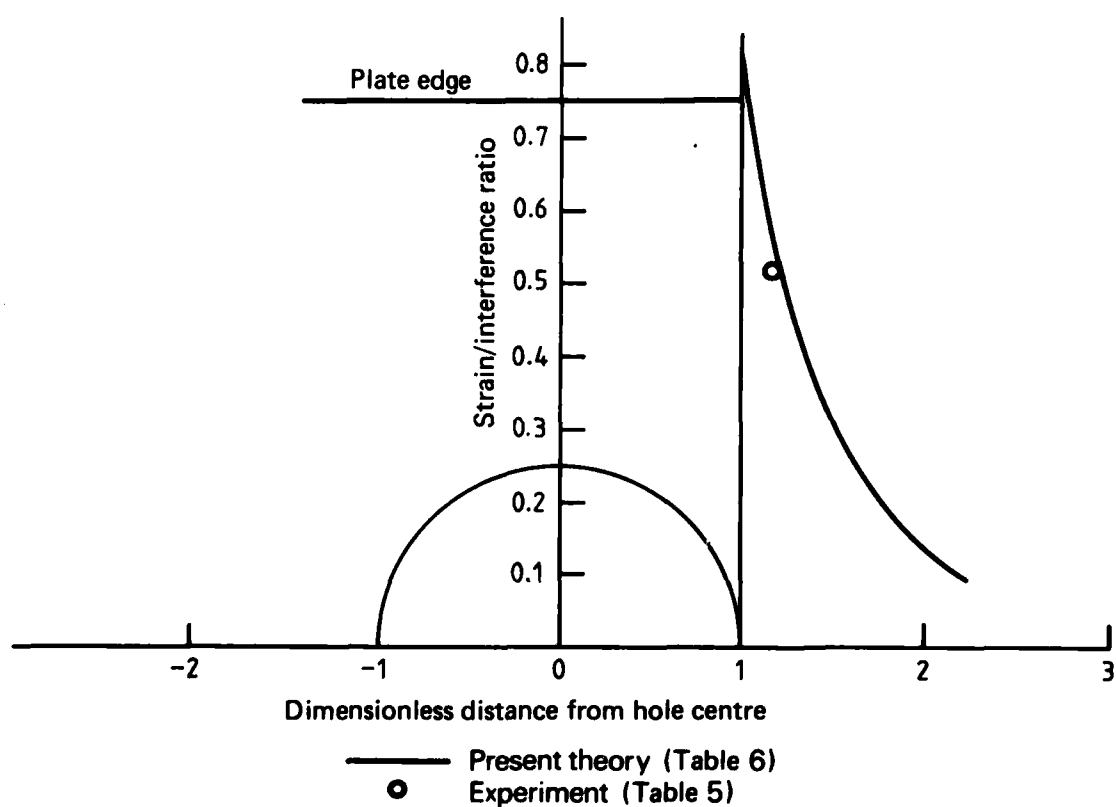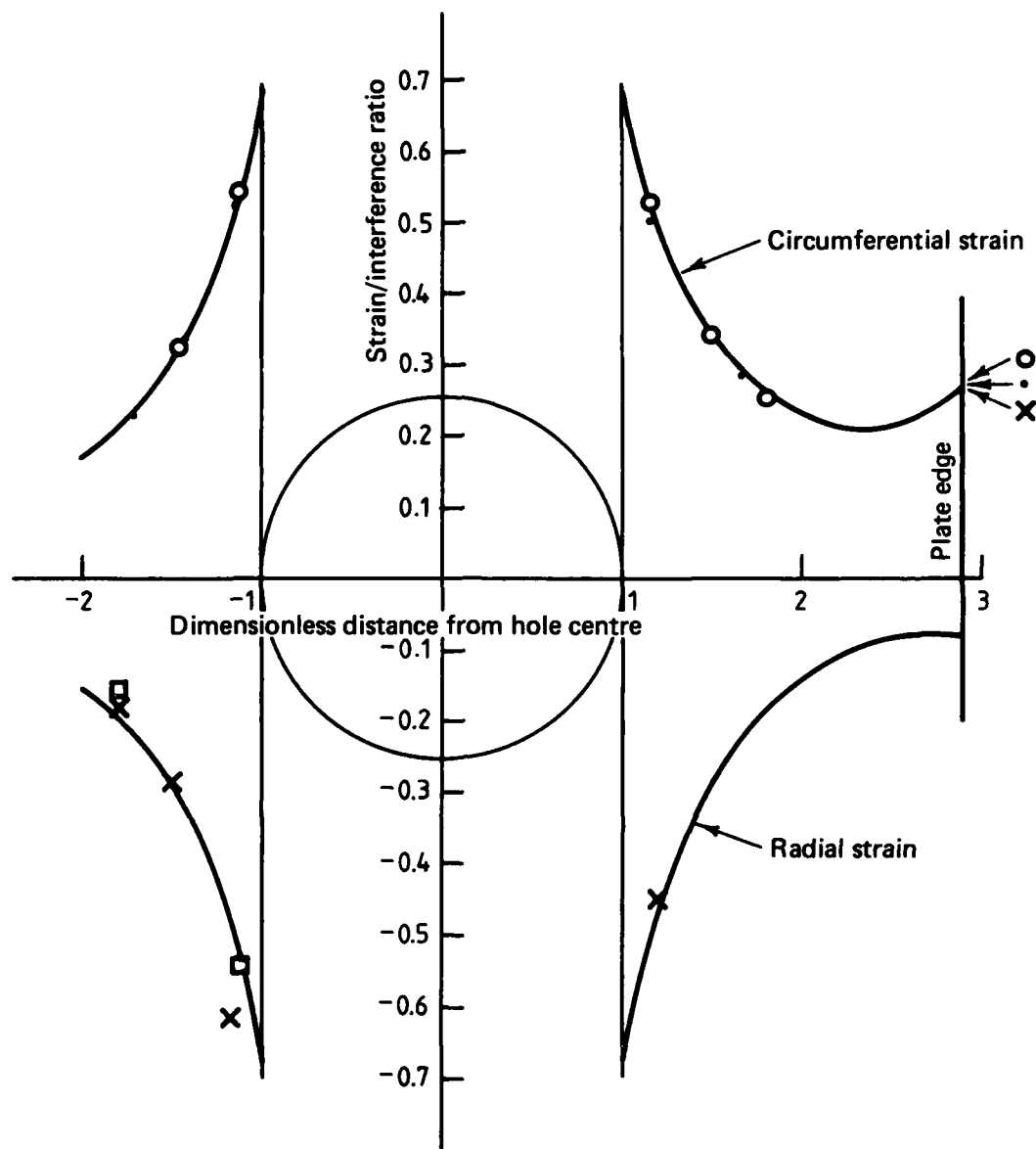
Radial strain

——— Present theory (Table 6)
Experimental values :
✕   Hole 4 } specimen 4/5 (Table 5)
•   Hole 5
☐   Hole 6 } specimen 6/7 (Table 5)
○   Hole 7

FIG. 14   STRAIN TRAVERSE PERPENDICULAR TO SPECIMEN EDGE —
CIRCUMFERENTIAL AND RADIAL STRAINS IN TWO-HOLE SPECIMEN.

FIG. 15   STRAIN TRAVERSE PARALLEL TO SPECIMEN EDGE — CIRCUMFERENTIAL
AND RADIAL STRAINS IN TWO-HOLE SPECIMENS

Air Force Office

Air Force Scientific Adviser
Aircraft Research and Development Unit
  Scientific Flight Group
  Library
Technical Division Library
RAAF Academy, Point Cook

Central Studies Establishment

Information Centre

DEPARTMENT OF DEFENCE SUPPORT

Government Aircraft Factories

Manager
Library

DEPARTMENT OF AVIATION

Library
Flying Operations and Airworthiness Division

STATUTORY AND STATE AUTHORITIES AND INDUSTRY

CSIRO
  Materials Science Division, Library
Trans-Australia Airlines, Library
Qantas Airways Limited
Ansett Airlines of Australia, Library
Commonwealth Aircraft Corporation, Library
Hawker de Havilland Aust. Pty Ltd, Bankstown, Library

UNIVERSITIES AND COLLEGES

Adelaide	Barr Smith Library
Flinders	Library
Latrobe	Library
Melbourne	Engineering Library
Monash	Hargrave Library
Newcastle	Library
Sydney	Engineering Library
N.S.W.	Physical Sciences Library
Queensland	Library
Tasmania	Engineering Library
Western Australia	Library
R.M.I.T.	Library

UNITED KINGDOM

Ministry of Defence, Research, Materials and Collaboration
CAARC, Secretary
Royal Aircraft Establishment
  Bedford, Library
National Physical Laboratory, Library
National Engineering Laboratory, Library
British Library, Lending Division
CAARC Coordinator, Structures
Rolls-Royce Ltd
  Aero Division Bristol, Library
British Aerospace
  Kingston-upon-Thames, Library
  Hatfield-Chester Division, Library

Universities and Colleges

Bristol	Engineering Library
Cambridge	Library, Engineering Department
London	Professor G. J. Hancock, Aero Engineering
Manchester	Professor N. Johannesen, Fluid Mechanics
Nottingham	Science Library
Southampton	Library
Strathclyde	Library
Cranfield Inst. of Technology	Library
Imperial College	Aeronautics Library

UNITED STATES OF AMERICA

NASA Scientific and Technical Information Facility
Applied Mechanics Reviews

Universities and Colleges

John Hopkins	Professor S. Corrsin, Engineering
Iowa	Professor R. I. Stephens
Illinois	Professor D. C. Drucker
Massachusetts Inst. of Technology	M.I.T. Libraries

SPARES (10 copies)

TOTAL (143 copies)

DOCUMENT CONTROL DATA

1. a. AR No. AR–003–012	1. b. Establishment No. ARL–STRUC–R–400	2. Document Date March, 1984	3. Task No. DST 83/005

4. Title STRAINS IN AN ELASTIC PLATE CONTAINING AN INTERFERENCE-FIT BOLT NEAR A FREE EDGE	5. Security a. document Unclassified	6. No. Pages 14
	b. title c. abstract U. U.	7. No. Refs 3

8. Author(s) G. S. Jost R. P. Carey	9. Downgrading Instructions

10. Corporate Author and Address Aeronautical Research Laboratories, P.O. Box 4331, Melbourne, Vic., 3001	11. Authority (*as appropriate*) a. Sponsor c. Downgrading b. Security d. Approval

12. Secondary Distribution (*of this document*

Approved for public release

Overseas enquirers outside stated limitations should be referred through ASDIS, Defence Information Services Branch, Department of Defence, Campbell Park, CANBERRA, ACT, 2601.

13. a. This document may be ANNOUNCED in catalogues and awareness services available to . . .

No limitations

13. b. Citation for other purposes (*i.e. casual announcement*) may be (*select*) unrestricted (*or*) as for 13 a.

14. Descriptors		15. COSATI Group
Bolted joints Stress analysis Interference fitting Elasticity	Holes (openings)	11130 01030

16. Abstract

An approximation has been developed to permit the use of elastic theory for a pressurized hole near the edge of a semi-infinite plate to predict strains in one containing an interference-fit fastener. A comparison of measured plate strains and those predicted for such a situation shows good agreement.

This page is to be used to record information which is required by the Establishment for its own use but which will not be added to the DISTIS data base unless specifically requested.

16. Abstract (Contd)

17. Imprint
Aeronautical Research Laboratories, Melbourne

18. Document Series and Number	19. Cost Code	20. Type of Report and Period Covered
Structures Report 400	277050	

21. Computer Programs Used

—

22. Establishment File Ref(s)

—